PHYSICAL REVIEW C **76**, 022802(R) (2007)

# Neutron capture cross sections of $^{186}$Os, $^{187}$Os, and $^{189}$Os for the Re-Os chronology

M. Segawa,[1] T. Masaki,[1] Y. Nagai,[1] Y. Temma,[1] T. Shima,[1] K. Mishima,[1] M. Igashira,[2] S. Goriely,[3]
A. Koning,[4] and S. Hilaire[5]

[1]*Research Center for Nuclear Physics, Osaka University, Ibaraki, Osaka 567-0047, Japan*
[2]*Research Laboratory for Nuclear Reactors, Tokyo Institute of Technology, O-okayama, Tokyo 152-8550, Japan*
[3]*Institut d'Astronomie et d'Astrophysique, Université Libre de Bruxelles, Campus de la Plaine, CP226, B-1050 Brussels, Belgium*
[4]*Nuclear Research and Consultancy Group, P.O. Box 25, NL-1755 ZG Petten, The Netherlands*
[5]*CEA/DAM Ile-de-France, DPTA/Service de Physique Nucléaire, BP 12, F-91680 Bruyères-le-Châtel, France*

(Received 9 March 2007; revised manuscript received 8 July 2007; published 30 August 2007)

Discrete as well as continuum $\gamma$-ray energy spectra from the neutron capture by $^{186}$Os, $^{187}$Os, and $^{189}$Os have been taken for the first time at $5 \leqslant E_n \leqslant 90$ keV by an anti-Compton NaI(Tl) spectrometer. The detection of a weak discrete $\gamma$-ray, about 0.5% of total $\gamma$-ray strength, demonstrates the high sensitivity of the present measurement. The energy spectra enabled us to accurately determine the reaction cross sections with a small systematic uncertainty. Based on the new cross sections, we reestimate on the basis of a careful reaction cross section calculation the correction factor $F_\sigma$ for the neutron capture on the 9.75-keV first excited state in $^{187}$Os as a function of stellar temperature, as required to derive the age of the galaxy within the Re-Os chronology.

DOI: 10.1103/PhysRevC.76.022802 PACS number(s): 25.40.Lw, 26.20.+f, 27.70.+q, 29.30.Kv

The duration of stellar nucleosynthesis is a subject of prime interest in astrophysics. It could provide valuable insight into the construction of cosmological models, as well as into the dating of the oldest stellar clusters, the formation of stars and galaxies, and the enrichment of the universe with heavy elements [1]. Although the half-life of $^{187}$Re is relatively long ($42.3 \pm 1.3$ Gyr [2]), the $^{187}$Re-$^{187}$Os pair has been considered to be one of the most reliable cosmo-chronometers to derive the age of the galaxy [3]. Indeed, $^{187}$Re is produced almost entirely by the rapid neutron capture ($r$-)process in stars [4] and both $^{186}$Os and $^{187}$Os are shielded from the $r$-process production, by $^{186}$W and $^{187}$Re, respectively. In addition, Os and Re have not been strongly fractionated from each other due to their similar geochemical properties. Knowing the decay rate of $^{187}$Re, the age of the Galaxy is derived by referring to the history of the $r$-process occurrence in the galaxy. In order to extract the abundance fraction of $^{187}$Os, due to the $^{187}$Re decay in meteorites, one must however correct for the production and depletion rates of $^{187}$Os by the slow ($s$-)neutron capture reactions of $^{186}$Os and of both the ground and 9.75 keV excited states of $^{187}$Os, respectively [5]. The former rate could be obtained using the local approximation of $\sigma_\gamma(A) \times N(A)$, where $\sigma_\gamma(A)$ and $N(A)$ are the neutron capture cross section of an $s$-process element with a mass number $A$ and its solar system abundance, respectively [6]. In order to constrain the destruction rate of $^{187}$Os through the excited state, the measurement of the neutron inelastic scattering cross section off the ground state of $^{187}$Os to the 9.75 keV ($J^\pi = 3/2^-$) state [7] and/or the neutron capture cross section of the ground state ($J^\pi = 3/2^-$) in $^{189}$Os were suggested [7]. In fact, the $^{187}$Os inelastic neutron scattering cross section was measured at several energies between 24 and 60 keV [8–11], and the $^{189}$Os neutron capture cross section [12,13] as well as the inelastic neutron scattering cross section to the 36.2 keV ($J^\pi = 1/2^-$) state [14] were measured. The neutron capture by the excited state in stellar environments is usually taken into account by introducing the correction factor $F_\sigma$ [15] given by

$$F_\sigma = \frac{\langle\sigma(186)\rangle^*}{\langle\sigma(186)\rangle_{\text{lab}}} \left\{ \frac{\langle\sigma(187)\rangle^*}{\langle\sigma(187)\rangle_{\text{lab}}} \right\}^{-1}, \tag{1}$$

where $\langle\sigma(A)\rangle_{\text{lab}}$ and $\langle\sigma(A)\rangle^*$ are the Maxwellian-averaged neutron capture cross sections (MACS) for $^A$Os in the ground state (as in the laboratory) and in stellar environments, respectively. Note that the local approximation mentioned above is claimed to be disturbed for $^{186}$Os and $^{187}$Os by the branchings at $^{185}$W and $^{186}$Re [4,16–20]. In fact, an overproduction of the $s$-only isotope $^{186}$Os by 20% is shown in the analysis of realistic $s$-process models in thermally-pulsing asymptotic giant branch stars. One of the proposed solutions for the overproduction problem is an increase in the neutron capture cross section of $^{186}$Os used in the models [4,17–20]. So far, the cross sections $\sigma_\gamma(^A\text{Os})$ have been measured for incident neutron energies $E_n$ such that $2.6 \leqslant E_n \leqslant 800$ keV for $A = 186$, 187, 188 [21], and 189 [12], and $0.5 \leqslant E_n \leqslant 150$ keV for $A = 186$–192 [13]. Uncertainties of about 30% exist between different data sets, leading to a relatively large range of predicted values of $F_\sigma$, i.e., $0.80 \leqslant F_\sigma \leqslant 1.15$ [9,21], hence to a large uncertainty in the determination of the galactic age. Note that the difference mentioned is larger than the reported uncertainty for each data, suggesting the existence of unidentified systematic uncertainties. The present paper aims at accurately improving $\sigma_\gamma(^A\text{Os})$ for $A = 186$, 187, and 189 with a small systematic uncertainty on the basis of a new experimental design. Here, we review what was learned from previous works. First, the enrichment of Os isotopes was rather low, namely 78–79% for $^{186}$Os, 70.4% for $^{187}$Os and 94.5% for $^{189}$Os. Second, previous capture cross section measurements on $^{189}$Os differ by 30% between different data sets. This difference, however, may not be due to an impurity contained in the $^{189}$Os sample, since this measurement was made using a highly enriched $^{189}$Os sample. It could come from

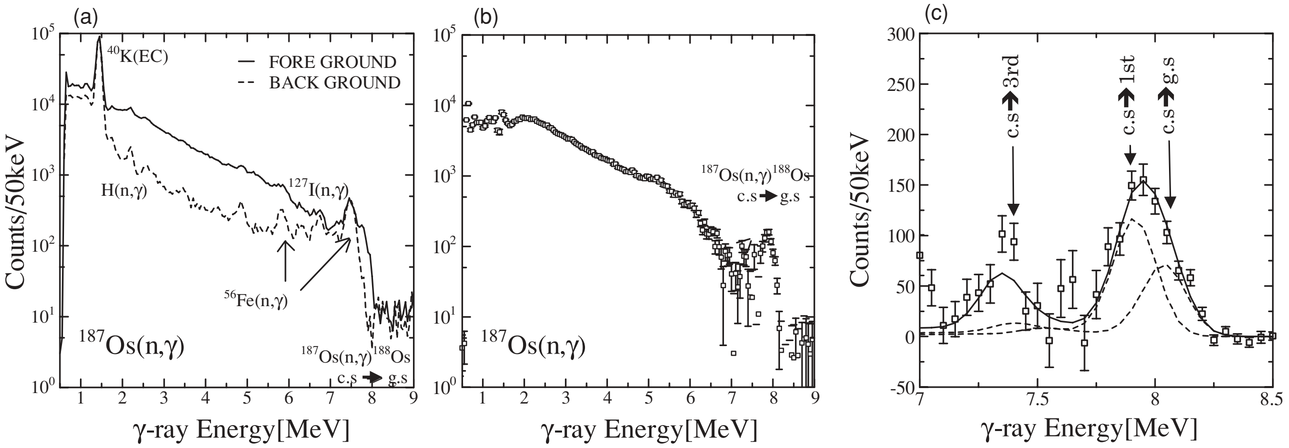

FIG. 1. (a) Foreground (including background) and background, and (b) background subtracted (net) $\gamma$-ray energy spectrum of the $^{187}$Os$(n,\gamma)^{188}$Os reaction. In the background spectrum $\gamma$-rays from the $^{56}$Fe$(n,\gamma)^{57}$Fe, H$(n,\gamma)^2$H, and $^{127}$I$(n,\gamma)^{128}$I reactions are observed. (c) is expanded in the region of discrete $\gamma$-rays in (b). A peak at about 8 MeV was composed of two peaks of 8.03 and 7.88 MeV $\gamma$-rays from the reaction to the ground ($J^\pi = 0^+$) and first excited stated ($J^\pi = 2^+$) of $^{188}$Os, respectively. Dotted lines indicate the experimental response function of the NaI(Tl) spectrometer of Ref. [23] fitted for 8.03 and 7.88 MeV $\gamma$-ray peaks, respectively. The solid line combines both dotted lines reproduces the peak at about 8 and 7.40 MeV nicely.

a systematic uncertainty due to the background subtraction for data, which were taken by using liquid scintillators $C_6F_6$ [12,21] and/or $C_6D_6$ [13]. Note that these detectors had a good time resolution, but could not resolve $\gamma$-ray energies. In the present study, an anti-Compton NaI(Tl) spectrometer and highly enriched samples are used to determine the $\gamma$-ray energy spectra from the $(n,\gamma)$ reaction on Os samples free from any uncertainties caused by a sample impurity. The use of a NaI(Tl) spectrometer allows us to detect the discrete $\gamma$-rays from the reaction to the low-lying states in $^{187}$Os, $^{188}$Os, and/or $^{190}$Os. Since a discrete $\gamma$-ray can be used to uniquely characterize a final nucleus, $^{187}$Os, $^{188}$Os, and/or $^{190}$Os, its detection is of vital importance to accurately determine $\sigma_\gamma(^A\mathrm{Os})$ with a small systematic uncertainty. In addition, the electromagnetic multipolarity of the $\gamma$-ray detected provides a direct insight on the neutron capture reaction mechanism. The experiment was carried out using pulsed keV neutrons from the $^7$Li$(p,n)^7$Be reaction. A pulsed proton beam was provided from the 3.2 MV Pelletron accelerator of the Research Laboratory for Nuclear Reactors at Tokyo Institute of Technology. We used a 0.402 g sample of $^{186}$Os, a 1.41 g sample of $^{187}$Os and 0.396 g sample of $^{189}$Os with 99.55%, 99.4% and 99.08% enrichment, respectively. A gold sample was used for normalization, since $\sigma_\gamma$(Au) is known with the small uncertainty of about 3% [22]. The NaI(Tl) spectrometer was set at 125.3° with respect to the proton beam direction [23], and therefore $\gamma$-ray intensities measured at this angle give angle-integrated intensities for a dipole transition. Time-of-flight (TOF) and $\gamma$-ray pulse height data taken by the NaI(Tl) spectrometer were stored on a hard disk in an event mode. Typical foreground including a background component, background, and background-subtracted (net) $\gamma$-ray spectra for $^{187}$Os$(n,\gamma)^{188}$Os at $10 \leqslant E_n \leqslant 90$ keV are for the first time obtained as shown in Figs. 1(a) and 1(b), respectively. In Fig. 1(b), we observed clearly a net $\gamma$-ray spectrum of $^{187}$Os$(n,\gamma)^{188}$Os free from background $\gamma$-rays due to the $(n,\gamma)$ reactions of $^{56}$Fe and $^{127}$I, and from the $\beta$-decay of $^{40}$K. In Fig. 1(c) we see discrete $\gamma$-rays of about 8 and 7.40 MeV from $^{187}$Os$(n,\gamma)^{188}$Os to low-lying states of $^{188}$Os. A $\gamma$-ray peak at about 8 MeV was composed of two peaks of 8.03 and 7.88 MeV to the ground ($J^\pi = 0^+$) and first ($J^\pi = 2^+$) excited states, respectively, and nicely fitted using the experimental response function of the NaI(Tl) spectrometer of [23], as shown in Fig. 1(c). We could not fit the peak as a single peak. The successful observation of the weak 8.03 MeV $\gamma$-ray, whose intensity is about 0.5% of the total $\gamma$-ray intensity, ensures that the $^{187}$Os$(n,\gamma)^{188}$Os reaction events are detected unambiguously with a good signal to noise ratio by properly subtracting any background events caused by neutron induced reactions by surrounding materials with a TOF method. Similarly, discrete $\gamma$-rays from the neutron capture by $^{186}$Os and $^{189}$Os to the ground state in $^{187}$Os and $^{190}$Os were clearly observed. A $\gamma$-ray yield in the net spectra thus obtained is derived by applying the pulse height weighting technique developed by Macklin and Gibbons [24] using the response function of the NaI(Tl) spectrometer. Using a $\gamma$-ray yield, $Y_\gamma(^A\mathrm{Os})$, the capture cross-section $\sigma_\gamma(^A\mathrm{Os})$ is given by

$$\sigma_\gamma(^A\mathrm{Os}) = \frac{T_{\mathrm{Au}}}{T_{\mathrm{A_{Os}}}}\frac{P_{\mathrm{A_{Os}}}}{P_{\mathrm{Au}}}\frac{C_{\mathrm{Au}}}{C_{\mathrm{A_{Os}}}}\frac{(r^2n)_{\mathrm{Au}}}{(r^2n)_{\mathrm{^AOs}}}\frac{Y_\gamma(^A\mathrm{Os})}{Y_\gamma(\mathrm{Au})}\sigma_\gamma(\mathrm{Au}). \quad (2)$$

In Eq. (2), $T_{\mathrm{Au}}$ and $P_{\mathrm{Au}}$ are the number of neutron counts measured by a $^6$Li-glass detector during the measurements of gold, and the neutron transmission of a gold sample, respectively; $r$ and $n$ are the radius and thickness (atoms/b) of the sample, respectively, $Y_\gamma$(Au) and $\sigma_\gamma$(Au) are the $\gamma$-ray yield and the absolute capture cross section for Au, respectively. A correction factor $C_{\mathrm{Au}}$ is introduced to correct for the overestimate of the $\gamma$-ray yield due to the multiple-scattering effect of, and of the shielding of the incident neutrons in a sample, respectively, and is calculated using the Monte Carlo code, TIME-MULTI [25]. The total cross sections

TABLE I. Cross sections expressed in barn for various neutron energies (in keV). For every cross section the accuracy is indicated between brackets.

| $E_n$ | $\sigma_\gamma(^{186}\mathrm{Os})$ | $E_n$ | $\sigma_\gamma(^{187}\mathrm{Os})$ | $E_n$ | $\sigma_\gamma(^{189}\mathrm{Os})$ |
|---|---|---|---|---|---|
| 18.8 | 0.57(3) | 8.1 | 2.81(16) | 5.6 | 3.27(11) |
| 31.0 | 0.41(3) | 13.2 | 1.94(7) | 8.1 | 2.72(9) |
| 39.8 | 0.40(2) | 19.6 | 1.38(5) | 13.2 | 1.93(5) |
| 52.7 | 0.34(2) | 25.0 | 1.19(4) | 19.5 | 1.42(4) |
| 70.5 | 0.35(2) | 31.0 | 1.02(3) | 25.0 | 1.14(4) |
| | | 39.8 | 0.95(3) | 31.0 | 1.09(3) |
| | | 52.5 | 0.80(3) | 39.6 | 0.89(3) |
| | | 73.4 | 0.65(2) | 52.6 | 0.73(2) |
| | | | | 73.9 | 0.59(2) |

for $^{186}$Os, $^{187}$Os, and $^{189}$Os are accurately obtained within an uncertainty of about 4% and given in Table I.

They are shown in Fig. 2 together with previously measured data and newly calculated values (see below). The quoted uncertainty given in the bracket is the result of combined uncertainties of the $\gamma$-ray yield statistics, and the absolute cross section of Au (3%), respectively. The uncertainties due to the response function of the NaI(Tl) spectrometer (2%) and the correction factor mentioned (3%) are negligibly small, since they cancel out by taking the ratio of each parameter, as given in Eq. (2). It should be pointed out that the present $\sigma_\gamma(^{187}\mathrm{Os})$ is larger than in previous measurements by 20–30% [13,21], and the $\sigma_\gamma(^{189}\mathrm{Os})$ is smaller than that of Ref. [13] by 20%. (The latter agrees with Ref. [12].) On the other hand, the present $\sigma_\gamma(^{186}\mathrm{Os})$ agrees with Refs. [13,21]. Different reasons for the discrepancy on the $^{187}$Os cross sections can be envisioned. First, the sensitivity of $\sigma_\gamma(^{187}\mathrm{Os})$ to the cross section $\sigma_\gamma(^{A}\mathrm{Os})$ contained in their samples $^{187}$Os(70%), $^{188}$Os(12.8%), $^{189}$Os(5.3%), $^{190}$Os(5.4%), $^{192}$Os(5.3%)} was calculated by changing $\sigma_\gamma(^{A}\mathrm{Os})$ by 20% to study the effect on their measured $\sigma_\gamma(^{187}\mathrm{Os})$ due to the low enrichment of $^{187}$Os samples used [12,13,21]. The calculated $\sigma_\gamma(^{187}\mathrm{Os})$ is not found to change significantly (about 2%), suggesting that the low enrichment of $^{187}$Os samples can not be a prime source of the mentioned discrepancy. Second, we paid attention to a difference of the neutron separation energy $S_n$ of a neutron capturing nucleus between $^{187}$Os (6.29 MeV) and $^{188}$Os (7.99 MeV), since in previous measurements the $\sigma_\gamma(^{A}\mathrm{Os})$ normalization was made using gold ($S_n = 6.51$ MeV) [12,21] and/or holmium ($S_n = 6.24$ MeV) [13]. Note that the derived $\sigma_\gamma(^{186}\mathrm{Os})$ agrees with the present $\sigma_\gamma(^{186}\mathrm{Os})$. Hence, the discrepancy could originate from observed events in previous data and/or an uncertainty of the weighting function in the $\gamma$-ray energy region from about 6.5 to 8 MeV. It is noteworthy that in a neutron capture experiment, an intense background $\gamma$-ray at 7.6 MeV from the neutron capture by iron, found in many places in a measurement room, is observed [see Fig. 1(a)]. An improper subtraction of such a high energy $\gamma$-ray background could cause the above-mentioned discrepancy, since a weighting function of a $\gamma$-ray detector increases significantly for higher $\gamma$-ray energies [24]. In addition, because of the characteristic feature of the weighting function mentioned, an uncertainty of the weighting function would cause a large error in obtaining $\sigma_\gamma(^{A}\mathrm{Os})$ for a nucleus with large $S_n$. The $\sigma_\gamma(^{A}\mathrm{Os})$ for a sample with $S_n \leqslant 6.5$ MeV could be determined rather free from uncertainties due to a background subtraction and/or due to a weighting function, since such uncertainties cancel out when considering the ratio given in Eq. (2). Here, it should be mentioned that the partial cross section for the $\gamma$-ray from $^{187}\mathrm{Os}(n,\gamma)^{188}\mathrm{Os}$ to the ground state of $^{188}$Os, $\sigma(n,\gamma)_{\mathrm{g.s.}}$, was for the first time obtained as 7.4 ± 1.6 mb at an average neutron energy $E_n = 42 \pm 1$ keV by analyzing the $\gamma$-ray yield in a wide neutron energy range from 10 to 90 keV to obtain a sufficient amount of the yield. The present $\sigma(n,\gamma)_{\mathrm{g.s.}}$ can be compared with the $^{188}$Os photodisintegration cross section leading to the ground state of $^{187}$Os, $\sigma(\gamma,n)_{\mathrm{g.s.}}$, using a principle of detailed balance. Recently the total $^{188}$Os photodisintegration cross section, $\sigma(\gamma,n)_{\mathrm{tot}}$, was measured at several photon energies between 7.3 and 10.9 MeV by Shizuma *et al.* [26]. The result at the average energy of $\langle E_\gamma \rangle = 8.04$ MeV with an uncertainty of 40 keV can be compared with the present result, as described below. Since the Q-value of $^{188}\mathrm{Os}(\gamma,n)^{187}\mathrm{Os}$ is 7.989 MeV, the neutrons emitted from the reaction at $\langle E_\gamma \rangle = 8.04$ MeV, corresponding to the neutron energy of 50.4 ± 40 keV, could reach all the states up to 75.0 keV in $^{187}$Os such as the ground, 9.75 keV, and 74.3 keV ones. Hence, the measured $\sigma(\gamma,n)_{\mathrm{tot}}$ at $E_\gamma = 8.04$ MeV gives the sum of the partial cross sections to these states. It is compared with the present $\sigma(n,\gamma)_{\mathrm{g.s.}}$ of 7.4 ± 1.6 mb at $E_n = 42$ keV by correcting for the neutron

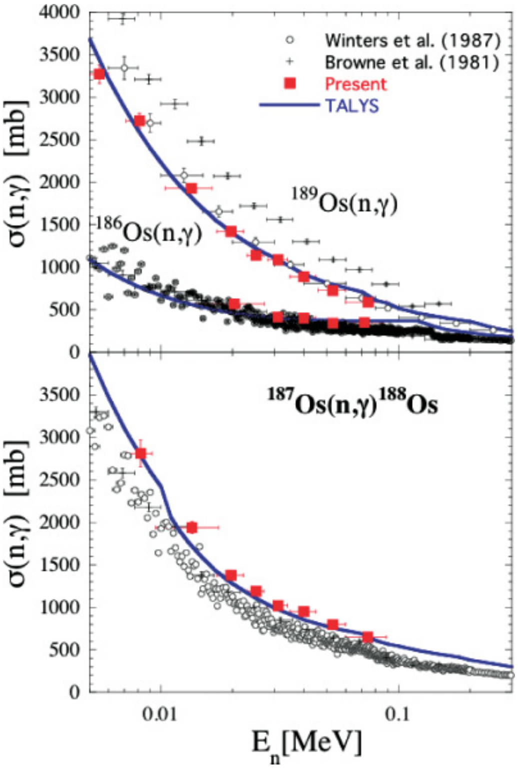

FIG. 2. (Color online) Comparison between measured (square) and calculated (solid line) cross sections for the $(n,\gamma)$ reactions on $^{186}$Os, $^{187}$Os, $^{189}$Os. Other symbols correspond to previous measurements, i.e., Winters *et al.* (open circles) [12] and Browne *et al.* (crosses) [13].

energy difference between two measurements by assuming the $1/v$ dependence of the $\sigma(n,\gamma)$. Note that the measured $\sigma(n,\gamma)$ was found to decrease with increasing the neutron energy, roughly in proportion to $1/v$, as given below in Fig. 2. The thus evaluated $\sigma(\gamma,n)_{\text{g.s.}}$ using the $\sigma(n,\gamma)$ is found to be 20 ± 13 mb, which agrees with the reported $\sigma(\gamma,n)_{\text{tot}}$ of 10.2 ± 1.5 ± 0.9 mb within the experimental uncertainty. Here, the uncertainty of the evaluated $\sigma(\gamma,n)_{\text{g.s.}}$ is dominated by the uncertainty of the average photon energy in [26], but not that of the present $\sigma(n,\gamma)_{\text{g.s.}}$. In fact, the relative uncertainty of the calculated $\sigma(\gamma,n)_{\text{g.s.}}$ is given as $\delta E_n/E_n$, which is 80% in the present case. The radiative cross sections for $A = 186$, 187, and 189 are now compared with calculation using the reaction code named TALYS [27,28]. The TALYS code takes into account all types of direct, preequilibrium and compound mechanisms to estimate the total reaction probability as well as the competition between the various open channels. All available experimental information on nuclear masses, deformation and spectra of low-lying states are considered whenever available. If not, global models for nuclear level formulas, $\gamma$-ray strength functions, and nucleon optical model potentials are considered to estimate the transmission coefficients. Details on the codes and the nuclear physics input can be found in Refs. [27,28]. Additional experimental data exist to constrain the nuclear input required to predict the present Os radiative capture cross section. These include $s$-wave resonance spacings at the neutron binding energy [29] as well as photodisintegration rate [30], and in particular the recent $^{188}$Os$(\gamma,n)^{187}$Os measurements with monoenergetic photons in the vicinity of the neutron separation energy which provide valuable information on the low-energy tail of the $\gamma$-ray strength function [26]. As well known, the radiative neutron capture cross section is extremely sensitive to the adopted model of nuclear level density. The model considered here is based on the combinatorial approach extensively described in Ref. [31]. This model corresponds to the first combinatorial calculation capable of reproducing experimental $s$-wave neutron spacings with an accuracy comparable to the one obtained with the analytical parametrized formula of the Back-Shifted-Fermi gas type. As prescribed in Ref. [31], the tabulated nuclear level density is fine-tuned with an empirical correction factor to reproduce at best the $s$-wave neutron spacings and the cumulative number of excited levels at low energies. The $\gamma$-ray strength function is determined within the Lorentzian-type approach to reproduce photoabsorption as well as photoneutron data [26,30,32]. The neutron capture cross sections obtained with the code TALYS are compared with the present experimental data in Fig. 2. In the particular case of $^{187}$Os, we also compare (Fig. 3) the inverse $^{188}$Os$(\gamma,n)^{187}$Os photodisintegration cross section obtained with exactly the same input physics as the one used to estimate $^{187}$Os$(n,\gamma)^{188}$Os cross section shown in Fig. 2. The stellar MACS for $^{186}$Os, $^{187}$Os, and $^{189}$Os are derived using the theoretical cross section adjusted on the present experimental data. Finally, on the basis of the present experimental data and the TALYS prediction of the contribution of the $^{187}$Os excited state to the radiative capture, the factor $F_\sigma$ can be estimated. The resulting stellar temperature $T$-dependence of $F_\sigma$ shown in Fig. 4 is seen to be lower than unity. At temperatures exceeding $10^8$ degrees, $F_\sigma$ is smaller than the value recently derived by Shizuma *et al.* [26]. With respect to the estimate of Ref. [26], our new lower value tend to increase the age of the galaxy, $T_G$, estimated on the basis of the Re-Os clock (see in particular, Fig. 9 of Ref. [33]). The impact of the different prediction for the $F_\sigma$ value on $T_G$ has been reestimated by [26] to about $\mathrm{d}T_G/\mathrm{d}F_\sigma = -(5\text{–}12)$ Gyr, which leads to an age difference of $\mathrm{d}T_G = 0.4\text{–}1$ Gyr between our new predictions and the one found by [33], if we assume that the $s$-process production of $^{187}$Os took place at an average temperature of about $10^8$ and $3 \times 10^8$ degrees, respectively. The difference between the various recent works provides an estimate of the uncertainty still affecting $F_\sigma$ which includes experimental measurements, as well as theoretical uncertainties in the nuclear reaction model and the various nuclear ingredients of relevance. The present $\sigma(n,\gamma)$ for $^{186}$Os and $^{187}$Os provides important information about the disturbance of the local approximation for the $s$-process Os isotopes mentioned above. In fact, the overproduction problem for $^{186}$Os is not considered to be due to the uncertainty of the $\sigma(n,\gamma)$ for $^{186}$Os used in the analysis [4,17], since the present $\sigma(n,\gamma)$ for $^{186}$Os agrees with previous data within the experimental uncertainty. The present $\sigma(n,\gamma)$ for $^{187}$Os, however, is larger than the previous data by about 20%, and therefore the local approximation would not be so much disturbed as claimed in the previous analysis [4,17]. A detailed analysis of the $s$-process yields for $^{186}$Os and $^{187}$Os using the

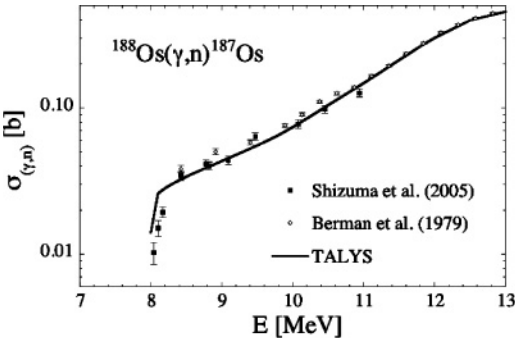

FIG. 3. Comparison between measured and calculated cross sections for the $(\gamma,n)$ reaction on $^{188}$Os [26].

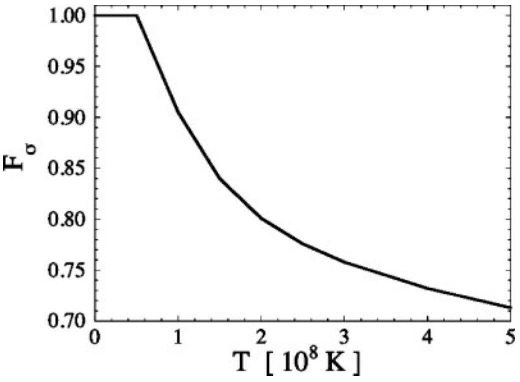

FIG. 4. Correction factor $F_\sigma$ obtained in the present study as a function of stellar temperature $T$.

present $\sigma(n, \gamma)$ is required. In summary, the first successful measurement of continuum as well as discrete $\gamma$-ray spectra from the neutron capture by $^{186,187,189}$Os at $5 \leqslant E_n \leqslant 90$ keV enables us to accurately determine the cross sections with a small systematic uncertainty. Using our new experimental constrained, the neutron capture cross section by the 9.75 keV first excited state in $^{187}$Os is calculated on the basis of the TALYS code. A new estimate of the crucial correction factor $F_\sigma$ has been derived as a function of the stellar temperature in order to put the Re-Os chronology on a better footing.

We would like to thank K. Takahashi for useful discussions, and K. Tosaka for his reliable operation of the Pelletron accelerator. This work was supported by a Grant-in-Aid for Scientific Research of the Japan Ministry of Education, Culture, Sports, Science, and Technology.

[1] E. M. Burbidge, G. R. Burbidge, W. A. Fowler, and F. Hoyle, Rev. Mod. Phys. **29**, 154 (1957).

[2] M. Linder *et al.*, Geochim. Cosmochim. Acta **53**, 1597 (1989).

[3] D. D. Clayton, Astrophys. J. **139**, 637 (1964).

[4] F. Käppeler, S. Jagg, Z. Y. Bao, and G. Reffo, Astrophys. J. **366**, 605 (1991).

[5] W. A. Fowler, Bull. Am. Astron. Soc. **4**, 412 (1972).

[6] J. Almeida and F. Käppeler, Astrophys. J. **265**, 417 (1983).

[7] W. A. Fowler, Rev. Mod. Phys. **56**, 149 (1984).

[8] R. L. Macklin, R. R. Winters, N. W. Hill, and J. A. Harvey, Astrophys. J. **274**, 408 (1983).

[9] R. L. Hershberger, R. L. Macklin, M. Balakrishnan, N. W. Hill, and M. T. McEllistrem, Phys. Rev. C **28**, 2249 (1983).

[10] L. L. Litvinskii, A. V. Murzin, and A. M. Shkarupa, Yad. Fiz. **56**, 31 (1993).

[11] L. L. Litvinskii, Y. A. Zhigalov, V. A. Libman, A. V. Murzin, and A. M. Shkarupa, Yad. Fiz. **58**, 206 (1995).

[12] R. R. Winters and R. L. Macklin, Astron. Astrophys. **171**, 9 (1987).

[13] J. C. Browne and B. L. Berman, Phys. Rev. C **23**, 1434 (1981).

[14] M. T. McEllistrem, R. R. Winters, R. L. Hershberger, Z. Cao, R. L. Macklin, and N. W. Hill, Phys. Rev. C **40**, 591 (1989).

[15] S. E. Woosley and W. A. Fowler, Astrophys. J. **233**, 411 (1979).

[16] M. Arnould, K. Takahashi, and K. Yokoi, Astron. Astrophys. **137**, 51 (1984).

[17] K. Sonnabend, P. Mohr, K. Vogt, A. Zilges, A. Mengoni, T. Rauscher, H. Beer, F. Käppeler, and R. Gallino, Astrophys. J. **583**, 506 (2003).

[18] P. Mohr *et al.*, Phys. Rev. C **69**, 032801(R) (2004).

[19] S. Muller, A. Kretschmer, K. Sonnabend, A. Zilges, and D. Galaviz, Phys. Rev. C **73**, 025804 (2006).

[20] B. S. Meyer and C. Wang, 38th Lunar and Planetary Science 38, March, 2007 in Texas, LPI Contribution No. 1338 (2007), p. 2055.

[21] R. R. Winters and R. L. Macklin, Phys. Rev. C **25**, 208 (1982).

[22] ENDF/B-VI data file for $^{197}$Au (MAT = 7925), evaluated by P. G. Young (1984).

[23] M. Igashira, K. Tanaka, and K. Masuda, *Proceedings of the Conference on the 8th International Symposium on Capture Gamma-Ray and Related Topics* (World Scientific, Singapore, 1993), p. 992.

[24] R. L. Macklin and J. H. Gibbons, Phys. Rev. **159**, 1007 (1967).

[25] K. Senoo, Y. Nagai, T. Shima, T. Ohsaki, and M. Igashira, Nucl. Instrum. Methods A **339**, 556 (1994).

[26] T. Shizuma, H. Utsunomiya, P. Mohr, T. Hayakawa, S. Goko, A. Makinaga, H. Akimune, T. Yamagata, M. Ohta, H. Ohgaki, Y. W. Lui, H. Toyokawa, A. Uritani, and S. Goriely, Phys. Rev. C **72**, 025808 (2005).

[27] A. J. Koning, S. Hilaire, and M. C. Duijvestijn, NRG report 21297/04, 62741/P (2004).

[28] A. J. Koning, S. Hilaire, and M. C. Duijvestijn, in *Proceedings of the International Conference on Nuclear Data for Science and Technology*, edited by C. Haight *et al.*, AIP Conf. Proc. No. 769 (AIP, New York, 2005), p. 1154.

[29] Handbook for calculations of nuclear reaction data Reference Input Parameter Library-2 IAEA-Tecdoc-1508 (2006).

[30] Photonuclear data for applications; cross sections and spectra IAEA-Tecdoc-1178 (2000).

[31] S. Hilaire and S. Goriely, Nucl. Phys. **A779**, 63 (2006).

[32] B. L. Berman, D. D. Faul, R. A. Alvarez, P. Meyer, and D. L. Olson, Phys. Rev. C **19**, 1205 (1979).

[33] K. Yokoi, K. Takahashi, and M. Arnould, Astron. Astrophys. **117**, 65 (1983).